

# Some surprising failures of Brueckner coupled cluster theory

Cite as: J. Chem. Phys. **112**, 7873 (2000); <https://doi.org/10.1063/1.481424>

Submitted: 04 January 2000 . Accepted: 17 February 2000 . Published Online: 24 April 2000

T. Daniel Crawford, and John F. Stanton



View Online



Export Citation

## ARTICLES YOU MAY BE INTERESTED IN

[Excited states from modified coupled cluster methods: Are they any better than EOM CCSD?](#)  
The Journal of Chemical Physics **146**, 144104 (2017); <https://doi.org/10.1063/1.4979078>

[An electron pair operator approach to coupled cluster wave functions. Application to He<sub>2</sub>, Be<sub>2</sub>, and Mg<sub>2</sub> and comparison with CEPA methods](#)

The Journal of Chemical Physics **74**, 4544 (1981); <https://doi.org/10.1063/1.441643>

[The equation of motion coupled-cluster method. A systematic biorthogonal approach to molecular excitation energies, transition probabilities, and excited state properties](#)

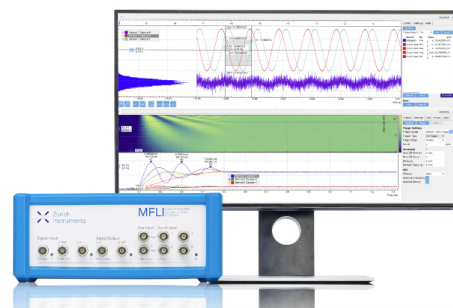
The Journal of Chemical Physics **98**, 7029 (1993); <https://doi.org/10.1063/1.464746>

## Challenge us.

What are your needs for periodic signal detection?



Zurich  
Instruments



## ARTICLES

## Some surprising failures of Brueckner coupled cluster theory

T. Daniel Crawford and John F. Stanton

*Institute for Theoretical Chemistry, Departments of Chemistry and Biochemistry,  
The University of Texas, Austin, Texas 78712-1167*

(Received 4 January 2000; accepted 17 February 2000)

Brueckner coupled cluster (B-CC) methods have seen a considerable rise in popularity over the last decade thanks, in part, to their apparent propensity for avoiding artifactual symmetry-breaking problems that sometimes plague Hartree-Fock-based approaches. Recent B-CC applications to problematic systems such as the tetraoxygen cation have provided encouraging examples of the success of this theory. In the present work, we examine the performance of the Brueckner technique for a number of other well-known symmetry-breaking problems, including the formylxyl radical, the first excited state of NO<sub>2</sub> and the nitrate radical. In these cases, B-CC methods are found to fail dramatically, predicting broken-symmetry equilibrium geometries in conflict with experimental and/or higher-level theoretical results. A framework is developed which indicates that these errors can be attributed to artificially exaggerated second-order Jahn-Teller interactions with nearby electronic states. Hence, in spite of their initial successes, Brueckner methods cannot be considered a panacea for symmetry-breaking problems. © 2000 American Institute of Physics.

[S0021-9606(00)30718-8]

### I. INTRODUCTION

Quantum chemical calculations are sometimes plagued by problems classified as spatial symmetry breaking,<sup>1</sup> in which the model electronic wave function (in the absence of appropriate constraints) fails to transform as an irreducible representation of the point group associated with the nuclear framework. The presence of a symmetry-breaking instability in approximate wave functions can yield qualitatively incorrect predictions of molecular properties; dozens of examples of anomalous equilibrium structures, harmonic vibrational frequencies, infrared intensities, etc., may be found in the literature.<sup>2-10</sup> Hartree-Fock (HF) wave functions are often susceptible to such errors, especially when applied to open-shell molecules. A number of studies in the last decade have indicated that even highly correlated methods can yield nonsensical results for problems of this type.<sup>11</sup>

A typical solution to symmetry-breaking problems is to use a multiconfigurational treatment, such as the now-classic example of the 2×2 nonorthogonal configuration interaction (CI) approach utilized by Jackels and Davidson in their pioneering work on low-lying doublet states of NO<sub>2</sub>.<sup>2</sup> Unfortunately, even multireference approaches do not provide a completely reliable solution to these problems without a careful analysis of the most appropriate active space.<sup>3,5,12</sup> Furthermore, traditional multireference approaches are often much more expensive than their single-reference counterparts and, for many high-level dynamic correlation methods such as coupled cluster (CC), are still too poorly developed for general application.

An alternative approach to symmetry-breaking problems

which has seen a considerable rise in popularity in the past 10 years is the Brueckner coupled cluster (B-CC) method,<sup>6,13-17</sup> in which the molecular orbitals are defined such that all single-excitation cluster amplitudes are zero. This scheme is designed to incorporate the most important relaxation effects associated with electron correlation directly into the orbitals. Although it does not follow that Brueckner orbitals are *a priori* immune to symmetry-breaking instabilities, a number of recent studies have indicated that B-CC methods appear to have a proclivity for maintaining symmetry in the electronic wave function and providing qualitatively correct predictions of corresponding molecular properties.<sup>6-8,10</sup>

Here we report the results of a number of applications of CC and B-CC theory to several well-known symmetry-breaking problems, including the  $\tilde{A}^2B_2$  state of NO<sub>2</sub>, the ground  $^2A'$  state of NO<sub>3</sub>, and the lowest  $\sigma$  radical of HCO<sub>2</sub>. Unfortunately, our findings indicate that, although spatial symmetry of the wave function is maintained for these examples, Brueckner methods give a qualitatively incorrect description of the associated potential energy surfaces. Hence, in spite of its initial success, B-CC theory cannot be considered a panacea for this class of problems.

### II. SYMMETRY-BREAKING TEST APPLICATIONS

The molecular properties for the various open-shell electronic states examined here were computed using coupled cluster methods with a number of different basis sets. For  $\tilde{X}^2B_2$  HCO<sub>2</sub>, an atomic natural orbital basis set, denoted ANO, was used, consisting of a set of general contractions—

TABLE I. Coupled cluster and CASPT2 predictions of structural data (bond lengths in Å and angles in degrees), harmonic vibrational frequencies (in  $\text{cm}^{-1}$ ), and infrared transition intensities (in parentheses in  $\text{km/mol}$ ) for the  ${}^2B_2$  state of formyloxyl  $\text{HCO}_2$  using an  $(14s9p4d)/[4s3p2d]/(8s4p)/[3s2p]$  ANO basis.

Property	CCSD		CCSD(T)		EOMIP-CCSD	CASPT2 <sup>a</sup>	Expt. <sup>b</sup>
	UHF	Brueckner	UHF	Brueckner			
$r(\text{C-H})$	1.085	1.085	1.087	1.087	1.084	1.092	
$r(\text{C-O})$	1.252	1.249	1.260	1.260	1.252	1.263	
$\theta(\text{H-C-O})$	123.8	123.8	123.7	123.7	123.7	123.5	
$\omega_1(a_1)$	3127 (31)	3129 (31)	3106 (29)	3103	3154 (21)	3053	3211
$\omega_2(a_1)$	1506 (62)	1522 (64)	1457 (49)	1457	1504 (62)	1437	1450
$\omega_3(a_1)$	651 (21)	657 (22)	636 (21)	636	659 (25)	624	550
$\omega_4(b_1)$	1072 (0)	1011 (3)	1017 (0)	1011	1045 (0)	1008	
$\omega_5(b_2)$	1300 (99)	1298 (92)	1276 (84)	1270	1304 (95)	1287	
$\omega_6(b_2)$	1165 (56)	841i (2821)	1076 (120)	889	1045 (199)	1150	

<sup>a</sup>Reference 19.

<sup>b</sup>Reference 56.

$(14s9p4d)/[4s3p2d]$  for carbon and oxygen and  $(8s4p)/[3s2p]$  for hydrogen—as constructed by Widmark, Malmqvist, and Roos.<sup>18</sup> This basis set is the same as that used in earlier CASSCF and CASPT2 calculations on formyloxyl radicals.<sup>19</sup> For  $\tilde{X}^2A_2'$   $\text{NO}_3$ , a double-zeta basis, denoted DZP1, was used, consisting of Dunning's contractions<sup>20</sup>— $(9s5p)/[4s2p]$  for nitrogen and oxygen—of Huzinaga's primitive Gaussian basis sets<sup>21</sup> with a set of polarization functions on each atom.<sup>22</sup> For the  $\tilde{A}^2B_2$  state of  $\text{NO}_2$ , a similar double-zeta type basis was used, consisting of the same set of Huzinaga/Dunning contracted Gaussian functions as DZP1, but with a different set of  $d$ -type polarization functions on nitrogen and oxygen [ $\alpha_d(\text{N})=0.80$  and  $\alpha_d(\text{O})=0.85$ ]. This basis is denoted DZP2 and was chosen to conform to earlier CASSCF calculations on this same state of  $\text{NO}_2$ .<sup>23</sup> Pure angular momentum functions were used for all  $d$ -type orbitals in all three basis sets.

Several different reference wave functions were used with the coupled cluster methods. For UHF and ROHF reference functions, the coupled cluster singles and doubles (CCSD) method,<sup>24,25</sup> CCSD including a perturbative estimate of the effects of connected triple excitations [CCSD(T)],<sup>26–28</sup> and full singles, doubles, and triples (CCSDT)<sup>29–31</sup> were used. For the Brueckner reference functions, since single excitation amplitudes are zero by construction, the analogous B-CCD,<sup>14,16</sup> B-CCD(T),<sup>6,16</sup> and B-CCDT<sup>32</sup> approaches were used. In addition, an equation-of-motion coupled cluster technique known as EOMIP-CCSD was used.<sup>33–42</sup> This method is designed for doublet radicals obtained *via* ionization from a closed-shell state (an anion in each of the cases studied here) and has certain advantages for the class of problems studied here. Specifically, it avoids the orbital instability problems observed in Hartree-Fock-based coupled cluster methods<sup>43–45</sup> and includes nondynamical correlation effects.

Geometry optimizations were carried out using our recently implemented open-shell analytic energy gradients for the B-CCD method<sup>16,46,47</sup> as well as for all UHF- and ROHF-based CCSD and CCSD(T) methods<sup>28,48</sup> and the EOMIP-CCSD method.<sup>28,49</sup> With B-CCD(T), B-CCDT,

and UHF-CCSDT,<sup>16,32</sup> gradients were computed using finite differences of energies. The geometry optimizations were considered to have converged once the root-mean-square of the internal coordinate forces fell below a threshold of  $1.0 \times 10^{-5} E_h/a_0$ . Harmonic vibrational frequencies and infrared intensities were computed using analytic energy second derivatives for UHF-CCSD and UHF-CCSD(T) methods,<sup>50–52</sup> finite differences of analytic energy gradients for ROHF-CCSD, ROHF-CCSD(T), B-CCD, and EOMIP-CCSD methods, and finite differences of energies for B-CCD(T), B-CCDT, and UHF-CCSDT. All computations were carried out with a local version of the ACESII package of quantum chemical programs.<sup>53</sup>

### A. $1^2B_2$ $\text{HCO}_2$

For more than 15 years, the  $\sigma$  and  $\pi$  formyloxyl radicals have been carefully scrutinized theoretically<sup>4,19,44,49,54,55</sup> not only because of their potential importance in combustion chemistry, but also because of the numerous difficulties associated with accurate determination of their spectroscopic properties. For the  $\sigma$  radicals, which are associated with the lowest  ${}^2B_2$  and  ${}^2A_1$  electronic states, the points of contention include whether the two states represent minima on the potential energy surface and which lies lower in energy. Many of the most thorough theoretical studies reported in the literature<sup>4,19,54,55</sup> make use of multiconfigurational self-consistent-field (MCSCF) or complete active space self-consistent-field (CASSCF) reference wave functions and account for dynamic electron correlation effects using either configuration interaction (MCSCF-CI and  $2 \times 2$  nonorthogonal CI) or second-order perturbation theory (CASPT2). In all such studies, the equilibrium geometry of the  ${}^2B_2$  electronic state is predicted to have  $C_{2v}$  symmetry, though some controversy still remains as to whether the  ${}^2A_1$  or  ${}^2B_2$  state lies lower in energy. These results are supported by ionized-state equation-of-motion coupled cluster (EOMIP-CC) computations,<sup>38,44,49</sup> which utilize as a reference the coupled cluster singles and doubles (CCSD) model wave function describing the anion,  $\text{HCO}_2^-$ . The latter approach offers a balanced treatment of the two states at geometries that allow

TABLE II. Coupled cluster predictions of the bond length (in Å), harmonic vibrational frequencies (in  $\text{cm}^{-1}$ ), and infrared transition intensities (in parentheses in  $\text{km/mol}$ ) for the  $\tilde{X}^2A'_2$  state of  $D_{3h}$ -symmetry  $\text{NO}_3$  using the DZP1 basis.

	CCSD		CCSD(T)		EOMIP-CCSD	Expt.
	UHF	Brueckner	UHF	Brueckner		
$r(\text{N-O})$	1.236	1.234	1.248	1.249	1.237	1.240 <sup>a</sup>
$\omega_1(a'_1)$	1158 (0)	1171 (0)	1093 (0)	1089	1150 (0)	1060 <sup>b,c</sup>
$\omega_2(a'_2)$	804 (13)	809 (13)	764 (9)	763	796 (12)	762 <sup>d,c</sup>
$\omega_3(e')$	1261 (38)	947 (41)	1138 (0)	1099	1146 (2)	1480 <sup>b,c</sup>
$\omega_4(e')$	409 (6)	991i (849)	342 (15)	20i	246 (23)	ca. 250 <sup>e,f</sup>

<sup>a</sup>Reference 60.

<sup>b</sup>Reference 59.

<sup>c</sup>Fundamental frequency.

<sup>d</sup>Reference 61.

<sup>e</sup>Reference 62.

<sup>f</sup>See Ref. 63.

for mixing of their unperturbed wave functions, a feature that makes it quite reliable for this class of problems.<sup>39,42</sup>

Table I summarizes the geometries, harmonic vibrational frequencies, and infrared transition intensities for the  $^2B_2$  state of  $\text{HCO}_2$  as computed using a variety of coupled cluster methods. As is usually expected, a given correlation treatment yields very similar geometric parameters, regardless of the chosen reference determinant. Indeed, to the number of decimal places reported in the table, the B-CCD(T) and UHF-CCSD(T) methods give identical results. This insensitivity is also observed for most of the harmonic vibrational frequencies and associated intensities; the UHF and Brueckner treatments give essentially the same results and compare well with the limited data available from experiment.<sup>56</sup> Of note, however, is the substantial disagreement between UHF-CC and B-CC results for  $\omega_6$ , which corresponds to the  $b_2$ -symmetry C-O antisymmetric stretching vibration. While the UHF-based coupled cluster, EOMIP-CCSD and CASPT2 methods agree with previous studies that the equilibrium geometry should have  $C_{2v}$  symmetry, the Brueckner-orbital CCD results predict instead that the  $C_{2v}$  stationary point is a transition state and that the true equilibrium geometry has only  $C_s$  symmetry. Inclusion of triple-excitation effects *via* the (T) correction, however, corrects this error; B-CCD(T) gives an antisymmetric stretching vibrational frequency which is in at least qualitative agreement with its UHF-CCSD(T) counterpart, although it remains somewhat lower. Since CASPT2, EOMIP-CCSD, and the UHF-based CC methods all have rather distinct parametrizations, the relatively good agreement of  $\omega_6$  predicted by these approaches strongly suggests that the exact value (with the present basis) is very likely in the range 1000–1200  $\text{cm}^{-1}$ .

## B. $\tilde{X}^2A'_2$ $\text{NO}_3$

The geometrical symmetry of the ground state of the nitrate radical has long presented an intriguing problem. Three structures have been found to be energetically most favorable: (a) a high-symmetry  $D_{3h}$  structure, (2) a  $C_{2v}$  structure with one long and two short N-O bonds (1L2S), and (3) a  $C_{2v}$  structure with one short and two long N-O bonds (1S2L), which is occasionally predicted to be the transition state for pseudorotation between equivalent 1L2S structures. While recent experimental analyses seem to agree

that the  $D_{3h}$  structure is energetically most favored, theoretical studies have again given conflicting results. MCSCF studies from the 1980s predicted that the Y-shaped structure (2) is the global minimum,<sup>57,58</sup> while more recent studies that include both dynamic and nondynamic electron correlation such as EOMIP-CCSD<sup>39</sup> predict that the  $D_{3h}$  structure is the global minimum. In 1992, Stanton, Gauss, and Bartlett reported that the B-CCD method placed  $C_{2v}$  structure (2) [optimized at the quasirestricted-Hartree-Fock CCSD (QRHF-CCSD) level<sup>25</sup>] slightly lower in energy (by ca. 2.5 kcal/mol) than the QRHF-CCSD  $D_{3h}$  structure, but B-CCD(T) reversed this ordering placing the high symmetry structure 0.5 kcal/mol lower.

Table II summarizes the computed properties of the ground  $^2A'_2$  state of  $\text{NO}_3$ . Once again, the expected approximate invariance of coupled cluster methods with respect to the choice of reference determinant is observed for the N-O bond length and the totally symmetric harmonic vibrational frequency, which agrees reasonably well with experimental results.<sup>59–62</sup> However, the  $e'$  harmonic vibrational frequency corresponding to the motion leading to the Y-shaped  $C_s$  structure differs substantially between the two methods. Again B-CCD predicts that the  $D_{3h}$  structure is a saddle point on the potential energy surface. When the level of theory is improved to include the effects of connected triple excitations *via* the (T) correction, the value of the UHF-CC  $e'$  frequency drops by approximately 70  $\text{cm}^{-1}$ . The corresponding B-CC triples correction, on the other hand, is substantial; the resulting frequency of 20i  $\text{cm}^{-1}$  indicates that the B-CCD(T) potential surface is extremely flat. While it is clear that the harmonic frequencies for the troublesome  $e'$  mode calculated with EOMIP-CCSD and UHF-based coupled cluster methods agree very well with the value of ca. 250  $\text{cm}^{-1}$  for  $\omega_4$  inferred from the photoelectron experiments of Weaver and co-workers,<sup>62,63</sup> such a comparison is compromised by the limited basis set used here.

## C. $\tilde{A}^2B_2$ $\text{NO}_2$

Historically, the first excited state of  $\text{NO}_2$  is the most studied of all the cases examined here. The careful theoretical work of Jackels and Davidson published more than two decades ago<sup>2</sup> provides a detailed description of the numerous complications associated with this electronic state, including

TABLE III. Coupled cluster and CASSCF predictions of structural data (bond lengths in Å and angles in degrees), harmonic vibrational frequencies (in  $\text{cm}^{-1}$ ), and infrared transition intensities (in parentheses in  $\text{km/mol}$ ) for the  $\tilde{A}^2B_2$  state of  $\text{NO}_2$  using the DZP2 basis set.

	CCSD		CCSD(T)		CCSDT		EOMIP-CCSD	CASSCF
	UHF	Brueckner	UHF	Brueckner	UHF	Brueckner		
$r(\text{N-O})$	1.269	1.266	1.281	1.281	1.282	1.280	1.269	1.281
$\theta(\text{O-N-O})$	100.5	100.4	100.6	100.6	100.7	100.7	100.5	101.3
$\omega_1(a_1)$	1488 (13)	1513 (13)	1410 (9)	1410	1407	1420	1491 (12)	1387 (8)
$\omega_2(a_1)$	760 (6)	769 (6)	733 (6)	735	730	735	763 (7)	729 (6)
$\omega_3(b_2)$	859 (16)	888i (1665)	815 (0)	781	775	498	821 (13)	325 (111)

a second-order Jahn–Teller interaction with the ground  $^2A_1$  state. The multireference configuration interaction (MRCI) computations reported by Jackels and Davidson predict that the  $\tilde{A}$  state has no stable minimum-energy structure, and instead collapses to the ground state *via* a pseudorotation through  $C_s$  geometries.<sup>2</sup> These results are supported by the more recent MRCI computations of Hirsch, Buenker, and Petrongolo,<sup>64</sup> CASSCF computations by Burton and co-workers<sup>23</sup> and EOMIP-CCSD computations by Kaldor<sup>39</sup> (later elaborated by Saeh and Stanton<sup>45</sup>), however, indicate that the  $C_{2v}$  structure is stable, but there is still little agreement as to the magnitude of the antisymmetric stretching vibrational frequency. Reported values range from  $359 \text{ cm}^{-1}$  (Ref. 23) to  $840 \text{ cm}^{-1}$  (Ref. 45). Although only the fundamental bending frequency has been observed experimentally,<sup>65</sup> recent simulations by Mahapatra and co-workers<sup>66</sup> of the photodetachment spectrum of  $\text{NO}_2^-$  (Ref. 65) indicate that previous multireference treatments significantly overestimate the nonadiabatic coupling strength between the  $\tilde{X}$  and  $\tilde{A}$  states. This suggests that the equilibrium geometry does indeed possess  $C_{2v}$  symmetry and that the harmonic vibrational frequency for antisymmetric motion predicted by the CASSCF method ( $325 \text{ cm}^{-1}$ ) is underestimated.

Table III summarizes the properties of the  $^2B_2$  state of  $\text{NO}_2$  computed with various coupled cluster methods, including full CCSDT with both UHF and Brueckner reference determinants. Once again, excellent agreement between UHF and Brueckner references is observed for the geometries and totally symmetric harmonic vibrational frequencies. However, the B-CCD method predicts that the  $C_{2v}$  stationary point is unstable with respect to antisymmetric stretching of the N–O bonds ( $\omega_3 = 888i \text{ cm}^{-1}$ ) while the UHF-CCSD and EOMIP-CCSD methods indicate that this structure is a minimum ( $\omega_3 = 859$  and  $821 \text{ cm}^{-1}$ , respectively). When the effects of triple excitations are included, all methods reveal semiquantitative agreement:  $\omega_3$  for B-CCD(T) is  $781 \text{ cm}^{-1}$  and for UHF-CCSD(T) is  $815 \text{ cm}^{-1}$ , again suggesting that the “correct” value is near  $800 \text{ cm}^{-1}$ . At the full CCSDT level of theory, however, the difference between the UHF- and Brueckner-based methods for  $\omega_3$  increases to  $277 \text{ cm}^{-1}$ , suggesting that the apparently good estimate of  $\omega_3$  provided by B-CCD(T) is largely fortuitous.

### III. DISCUSSION

A common characteristic among the three problematic cases described above is the presence of a second electronic state of appropriate symmetry lying above and relatively close to the state of interest. In such cases, the two electronic states can undergo a second-order (pseudo) Jahn–Teller (SOJT) interaction along a particular nonsymmetric vibrational coordinate which allows them to mix. Nitrogen dioxide provides a simple example of this behavior. At the equilibrium geometry of the  $\tilde{A}^2B_2$  state, the ground  $^2A_1$  state lies somewhat higher in energy (the equilibrium bond angle of the latter is ca.  $134^\circ$ ; cf. Table III). The true SOJT interaction between the two perturbs the  $\tilde{A}$  state downwards along the  $b_2$  antisymmetric stretching coordinate. The questions which are relevant to the anomalous results reported in Tables I–III relate to the magnitude of the SOJT interaction and how it is manifested in coupled cluster computations of harmonic vibrational frequencies.

The single-reference coupled cluster energy may be written in its most general form as

$$E_{\text{CC}} = \langle 0 | \hat{\mathcal{L}} e^{-\hat{T}} \hat{H} e^{\hat{T}} | 0 \rangle \equiv \langle 0 | \hat{\mathcal{L}} \bar{H} | 0 \rangle, \quad (1)$$

where  $|0\rangle$  is the reference function (in this case, either a Hartree–Fock or a Brueckner determinant),  $\hat{T}$  is the usual ground-state cluster operator, and  $\hat{\mathcal{L}}$  is the cluster de-excitation operator of the corresponding left-hand state. The notation  $\bar{H}$  is often used as a shorthand for the similarity-transformed electronic Hamiltonian. For the CCSD method, the cluster operators are truncated to include only singly and doubly excited determinants,  $\hat{T} \equiv \hat{T}_1 + \hat{T}_2$ , while for Brueckner methods, the  $\hat{T}_1$  operator is identically zero at convergence. The equations defining the cluster amplitudes comprising the  $\hat{T}$  operators are obtained by requiring that the energy be stationary with respect to the linear parameters  $\hat{\mathcal{L}}$ ,<sup>67</sup>

$$\frac{\partial E_{\text{CC}}}{\partial \mathcal{L}_\phi} = \langle \phi | \bar{H} | 0 \rangle = 0. \quad (2)$$

In this expression,  $|\phi\rangle$  represents an excited Slater determinant and  $\mathcal{L}_\phi$  the  $\phi$ th component of the  $\mathcal{L}$  amplitudes. In the Hartree–Fock-based CCSD method, for example, two sets of (coupled, nonlinear) equations are obtained which involve projection onto singly ( $|\phi_1\rangle$ ) and doubly ( $|\phi_2\rangle$ ) excited de-

TABLE IV. Selected UHF–CCSD and Brueckner–CCD vertical electronic excitation energies [linear response (LR)] and electric response (ER) energies (see text) for several difficult molecular cases. The optimized geometry for the right-hand state at each level of theory was taken as the reference geometry. Energies are given in eV.

Molecule	Transition	Basis set	UHF–CCSDLR	B–CCDLR	B–CCDER
HCO <sub>2</sub>	( $\tilde{A}^2A_1 \leftarrow \tilde{X}^2B_2$ )	ANO	1.374	1.173	0.907
NO <sub>3</sub>	( $\tilde{A}^2E' \leftarrow \tilde{X}^2A_2'$ )	DZP1	2.021	1.826	1.466
NO <sub>2</sub>	( $\tilde{X}^2A_1 \leftarrow \tilde{A}^2B_2$ )	DZP2	0.901	0.647	0.406

terminants thus defining the  $\hat{T}_1$  and  $\hat{T}_2$  cluster amplitudes, respectively. For the Brueckner CCD method, the latter set of equations is retained (though the similarity transformation of  $\hat{H}$  involves only the  $\hat{T}_2$  cluster operators) and the  $\hat{T}_1$  equation is replaced by a similar one defining the orbital rotation parameters,  $\kappa$ .<sup>16,46</sup>

Quadratic force constants from which harmonic vibrational frequencies are computed may be determined directly from the analytic second derivative of the coupled cluster energy with respect to nuclear coordinates ( $\alpha$  and  $\beta$ ),<sup>50–52</sup>

$$\frac{\partial^2 E_{CC}}{\partial \alpha \partial \beta} = \langle 0 | \frac{\partial \hat{\mathcal{L}}}{\partial \beta} \bar{H}^\alpha | 0 \rangle + \langle 0 | \hat{\mathcal{L}} \bar{H}^{\alpha\beta} | 0 \rangle + \langle 0 | \hat{\mathcal{L}} \left[ \bar{H}^\alpha, \frac{\partial \hat{T}}{\partial \beta} \right] | 0 \rangle, \quad (3)$$

where  $\bar{H}^\alpha \equiv e^{-\hat{T}} (\partial \hat{H} / \partial \alpha) e^{\hat{T}}$  and  $\bar{H}^{\alpha\beta} \equiv e^{-\hat{T}} (\partial \hat{H} / \partial \alpha \partial \beta) e^{\hat{T}}$ . This expression, which is asymmetric in the perturbation coordinates  $\alpha$  and  $\beta$  for computational reasons,<sup>50</sup> depends on the derivatives of the amplitudes  $\partial \hat{T} / \partial \beta$  and  $\partial \hat{\mathcal{L}} / \partial \beta$ . These are determined by differentiating the amplitude-defining equations such as Eq. (2) with respect to nuclear coordinates. For the  $\hat{T}_1$  and  $\hat{T}_2$  amplitudes in the Hartree–Fock-based CCSD approach, for example, this leads to a set of coupled, linear equations for the perturbed amplitudes of the form

$$\begin{pmatrix} \frac{\partial^2 E_{CC}}{\partial \mathcal{L}_1 \partial T_1} & \frac{\partial^2 E_{CC}}{\partial \mathcal{L}_1 \partial T_2} \\ \frac{\partial^2 E_{CC}}{\partial \mathcal{L}_2 \partial T_1} & \frac{\partial^2 E_{CC}}{\partial \mathcal{L}_2 \partial T_2} \end{pmatrix} \begin{pmatrix} \frac{\partial T_1}{\partial \alpha} \\ \frac{\partial T_2}{\partial \alpha} \end{pmatrix} = - \begin{pmatrix} \frac{\partial^2 E_{CC}}{\partial \mathcal{L}_1 \partial I} \\ \frac{\partial^2 E_{CC}}{\partial \mathcal{L}_2 \partial I} \end{pmatrix} \frac{\partial I}{\partial \alpha}, \quad (4)$$

where  $I$  represents the Hamiltonian one- and two-electron integral components. For the B–CCD method, a similar equation is obtained in which all  $T_1$  terms are simply replaced by the orbital rotation parameters  $\kappa$ .

Formally, the perturbed cluster amplitudes  $\partial T / \partial \alpha$  (or perturbed orbital rotation parameters  $\partial \kappa / \partial \alpha$  for B–CC) required for the quadratic force constants in Eq. (3) are determined by inverting the matrix on the left-hand side of Eq. (4). As can be shown *via* simple differentiation of Eq. (2), the energy second derivatives appearing in this matrix may be written as

$$\frac{\partial^2 E_{CC}}{\partial \mathcal{L}_\phi \partial T_{\phi'}} = \langle \phi | (\bar{H} - E_{CC} \hat{1}) | \phi' \rangle. \quad (5)$$

In Hartree–Fock-based coupled cluster methods, the RHS of Eq. (5) is the equation of motion coupled cluster (EOM–CC)<sup>38</sup> or linear response (LR)<sup>68,69</sup> matrix, eigenval-

ues of which represent electronic excitation energies relative to the coupled cluster reference state energy,  $E_{CC}$ . The equations that determine the perturbed lambda amplitudes also involve formal inversion of the same matrix. It can be demonstrated that the second derivative of the energy with respect to a particular normal coordinate for Hartree–Fock-based coupled cluster methods contains terms of the usual form

$$\frac{\partial^2 E_{CC}}{\partial Q^2} \leftarrow \sum_J \frac{\tilde{\Psi}_{CC} | \partial \hat{H} / \partial Q | \Psi_{EOM}^J \rangle \langle \tilde{\Psi}_{EOM}^J | \partial \hat{H} / \partial Q | \Psi_{CC} \rangle}{E_{CC} - E_J} \quad (6)$$

which includes the left- and right-hand ground and excited state wave functions and energies, the latter in the corresponding EOM–CC approximation. Hence, if orbital relaxation effects are ignored (a good approximation if there is no nearly singularity in the orbital Hessian), SOJT interactions are accounted for in an apparently satisfactory way in these approaches, provided the EOM description of the *unperturbed* excited states is reasonably accurate and the ratio of vertical separation to coupling strength not too small.<sup>70</sup> This provides some justification for why standard coupled cluster methods (those that do not involve a coupling of orbital rotation and electron correlation parameters) appear to hold up quite well for the systems studied here.

In the corresponding Brueckner-based coupled cluster theory, however, the response matrix of Eq. (5) corresponds to the linear response of the wave function to a formally real perturbation (referred to here as the “electric Hessian”), rather than the appropriate complex time-dependent periodic perturbation required to determine electronic excitation energies.<sup>71,72</sup> This property of the B–CCD method arises as a result of the coupling between the orbital rotation and correlation procedures and bears considerable formal similarity to the distinction between the random phase approximation (RPA) for the determination of excitation energies at the Hartree–Fock level and coupled-perturbed Hartree–Fock (CPHF) theory. In that case, it is well known that the eigenvalues of the electric (molecular orbital) Hessian, determined *via* the CPHF equations, differ from the true excitations energies of the system.<sup>71</sup>

Table IV summarizes excitation energies calculated by UHF–EOM–CCSD and B–CCD linear responses as well as eigenvalues of the B–CCD electric Hessian matrix corresponding to the most important SOJT interactions in the four molecular examples given above. In these problematic cases, there is a substantial difference between electronic excitation

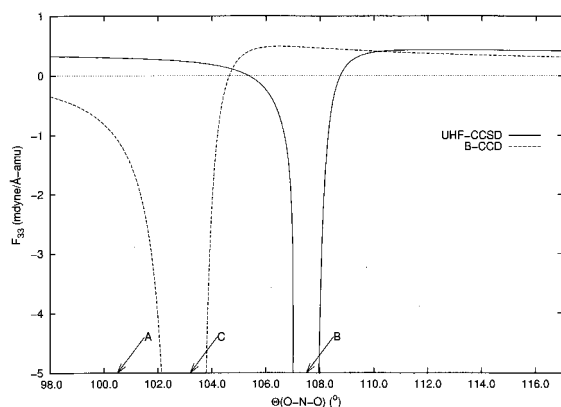


FIG. 1. DZP/UHF-CCSD and B-CCD quadratic force constants [polynomial fit to computed points (not shown)] for antisymmetric stretching in the  $\tilde{A}^2B_2$  state of  $\text{NO}_2$  as a function of O-N-O bond angle at fixed N-O lengths of 1.269 and 1.266 Å, respectively. Arrows on the horizontal axis indicate: (A) the UHF-CCSD and B-CCD equilibrium bond angle for the  $\tilde{A}^2B_2$  state, (B) the crossing point of the UHF-CCSD  $\tilde{A}^2B_2$  and UHF-EOM-CCSD  $\tilde{X}^2A_1$  energies, and (C) the crossing point of the B-CCD  $\tilde{A}^2B_2$  and B-CCD-ER  $\tilde{X}^2A_1$  energies.

energies given by the UHF-EOM-CCSD and B-CCD-LR methods, with the latter generally several tenths of an eV lower.<sup>73</sup> Most pertinent to the anomalous vibrational frequencies described earlier, however, is the significant difference between the UHF-EOM-CCSD eigenvalues and those of the B-CC electric Hessian [hereafter referred to as the “electric response” (ER)], with the latter lying 27% to 55% below the corresponding UHF-EOM-CCSD excitation energies. In the B-CCD method, it is these ER eigenvalues that play the role of excitation energies in modeling the SOJT effect.<sup>74</sup> The substantially smaller eigenvalues of the B-CC electric Hessian for these problematic cases is a principal cause of the apparent exaggeration of the SOJT effect.<sup>75</sup>

The mathematical behavior described above is clearly illustrated by the lowest two states of  $\text{NO}_2$ . Figure 1 depicts the UHF-CCSD and B-CCD force constants of the  $\tilde{A}^2B_2$  state as a function of O-N-O bond angle (at fixed N-O bond lengths of 1.269 and 1.266 Å, respectively), where arrows indicate the point at which the  $\tilde{A}^2B_2$  (UHF-CCSD or B-CCD) and  $\tilde{X}^2A_1$  (EOM-CCSD or B-CCD-ER) energies cross and the equilibrium bond angles. The  $\tilde{A}^2B_2$  state is lower than the  $\tilde{X}^2A_1$  to the left of the pole and higher to the right of it. For the UHF-based results at the equilibrium geometry, the gap between the two states is about 0.9 eV and a relatively narrow pole is centered at the point of degeneracy (approximately 107.5°), which is relatively far from the equilibrium bond angle of 100.5°. For the Brueckner-based methods, the singularity occurs quite close to the equilibrium bond angle (where the gap is only 0.4 eV), and the pole is significantly broader than that found at the UHF-CCSD level. The result is a qualitatively incorrect description of the antisymmetric stretching potential of the  $\tilde{A}^2B_2$  state at its minimum energy  $C_{2v}$  geometry.

## IV. CONCLUSIONS

Although Brueckner coupled cluster methods have been touted in recent years as a reliable approach for the avoidance of artifactual symmetry-breaking phenomena that are known to plague Hartree-Fock-based correlation treatments, we have discovered a number of cases for which B-CC methods fail dramatically, including the lowest  $^2B_2$  state of  $\text{HCO}_2$ , the nitrate radical, and the first excited state of  $\text{NO}_2$ . Each of these cases is characterized by a true second-order Jahn-Teller interaction between the state of interest and a nearby excited state. As illustrated by detailed computations on the  $\tilde{A}^2B_2$  state of nitrogen dioxide, the source of the B-CC errors appears to be an overemphasis of this second-order Jahn-Teller interaction, manifested in the near singularity of a Brueckner “electric” Hessian matrix. Hence, in spite of their initial success, Brueckner methods cannot be considered a cure-all for symmetry-breaking problems.

## ACKNOWLEDGMENTS

This research was sponsored by the Robert A. Welch Foundation, the National Science Foundation, and the Petroleum Research Fund. We thank W. D. Allen (Georgia) for his interest in this work and stimulating discussions.

- <sup>1</sup>E. R. Davidson and W. T. Borden, *J. Phys. Chem.* **87**, 4783 (1983).
- <sup>2</sup>C. F. Jackels and E. R. Davidson, *J. Chem. Phys.* **64**, 2908 (1976).
- <sup>3</sup>L. Engelbrecht and B. Liu, *J. Chem. Phys.* **78**, 3097 (1983).
- <sup>4</sup>A. D. McLean, B. H. Lengsfeld, J. Pacansky, and Y. Ellinger, *J. Chem. Phys.* **83**, 3567 (1985).
- <sup>5</sup>W. D. Allen, D. A. Horner, R. L. DeKock, R. B. Remington, and H. F. Schaefer, *Chem. Phys. Lett.* **133**, 11 (1989).
- <sup>6</sup>J. F. Stanton, J. Gauss, and R. J. Bartlett, *J. Chem. Phys.* **97**, 5554 (1992).
- <sup>7</sup>L. A. Barnes and R. Lindh, *Chem. Phys. Lett.* **223**, 207 (1994).
- <sup>8</sup>Y. Xie, W. D. Allen, Y. Yamaguchi, and H. F. Schaefer, *J. Chem. Phys.* **104**, 7615 (1996).
- <sup>9</sup>J. Hrušák and S. Iwata, *J. Chem. Phys.* **106**, 4877 (1997).
- <sup>10</sup>T. D. Crawford, J. F. Stanton, P. G. Szalay, and H. F. Schaefer, *J. Chem. Phys.* **107**, 2525 (1997).
- <sup>11</sup>T. D. Crawford, J. F. Stanton, W. D. Allen, and H. F. Schaefer, *J. Chem. Phys.* **107**, 10626 (1997).
- <sup>12</sup>A. Spielfiedel *et al.*, *J. Chem. Phys.* **97**, 8382 (1992).
- <sup>13</sup>R. K. Nesbet, *Phys. Rev.* **109**, 1632 (1958).
- <sup>14</sup>R. A. Chiles and C. E. Dykstra, *J. Chem. Phys.* **74**, 4544 (1981).
- <sup>15</sup>L. Z. Stolarczyk and H. J. Monkhorst, *Int. J. Quantum Chem., Symp.* **18**, 267 (1984).
- <sup>16</sup>N. C. Handy, J. A. Pople, M. Head-Gordon, K. Raghavachari, and G. W. Trucks, *Chem. Phys. Lett.* **164**, 185 (1989).
- <sup>17</sup>T. D. Crawford and H. F. Schaefer, in *Reviews in Computational Chemistry*, edited by K. B. Lipkowitz and D. B. Boyd (VCH, New York, 1999), Vol. 14, Chap. 2, pp. 33–136.
- <sup>18</sup>P.-O. Widmark, P.-A. Malmqvist, and B. O. Roos, *Theor. Chim. Acta* **77**, 291 (1990).
- <sup>19</sup>A. Rauk, D. Yu, P. Borowski, and B. Roos, *Chem. Phys. Lett.* **197**, 73 (1995).
- <sup>20</sup>T. H. Dunning, *J. Chem. Phys.* **53**, 2823 (1970).
- <sup>21</sup>S. Huzinaga, *J. Chem. Phys.* **42**, 1293 (1965).
- <sup>22</sup>L. T. Redmon, G. D. Purvis, and R. J. Bartlett, *J. Am. Chem. Soc.* **101**, 2856 (1979).
- <sup>23</sup>N. A. Burton, Y. Yamaguchi, I. L. Alberts, and H. F. Schaefer, *J. Chem. Phys.* **95**, 7466 (1991).
- <sup>24</sup>G. D. Purvis and R. J. Bartlett, *J. Chem. Phys.* **76**, 1910 (1982).
- <sup>25</sup>M. Rittby and R. J. Bartlett, *J. Phys. Chem.* **92**, 3033 (1988).
- <sup>26</sup>K. Raghavachari, G. W. Trucks, J. A. Pople, and M. Head-Gordon, *Chem. Phys. Lett.* **157**, 479 (1989).
- <sup>27</sup>R. J. Bartlett, J. D. Watts, S. A. Kucharski, and J. Noga, *Chem. Phys. Lett.* **165**, 513 (1990); **167**, 609(E) (1990).

- <sup>28</sup>J. Gauss, W. J. Lauderdale, J. F. Stanton, J. D. Watts, and R. J. Bartlett, *Chem. Phys. Lett.* **182**, 207 (1991).
- <sup>29</sup>J. Noga and R. J. Bartlett, *J. Chem. Phys.* **86**, 7041 (1987); **89**, 3401(E) (1988).
- <sup>30</sup>G. E. Scuseria and H. F. Schaefer, *Chem. Phys. Lett.* **152**, 382 (1988).
- <sup>31</sup>J. D. Watts and R. J. Bartlett, *J. Chem. Phys.* **93**, 6104 (1990).
- <sup>32</sup>J. D. Watts and R. J. Bartlett, *Int. J. Quantum Chem., Symp.* **28**, 195 (1994).
- <sup>33</sup>H. J. Monkhorst, *Int. J. Quantum Chem., Symp.* **11**, 421 (1977).
- <sup>34</sup>D. Mukherjee and P. K. Mukherjee, *Chem. Phys. Lett.* **39**, 325 (1979).
- <sup>35</sup>K. Emrich, *Nucl. Phys. A* **351**, 379 (1981).
- <sup>36</sup>S. Ghosh and D. Mukherjee, *Proc.-Indian Acad. Sci., Chem. Sci.* **93**, 947 (1984).
- <sup>37</sup>H. Sekino and R. J. Bartlett, *Int. J. Quantum Chem., Symp.* **18**, 255 (1984).
- <sup>38</sup>J. F. Stanton and R. J. Bartlett, *J. Chem. Phys.* **98**, 7029 (1993).
- <sup>39</sup>U. Kaldor, *Theor. Chim. Acta* **80**, 427 (1991).
- <sup>40</sup>D. Mukhopadhyay, S. Mukhopadhyay, R. Chaudhuri, and D. Mukherjee, *Theor. Chim. Acta* **80**, 441 (1991).
- <sup>41</sup>C. M. L. Rittby and R. J. Bartlett, *Theor. Chim. Acta* **80**, 469 (1991).
- <sup>42</sup>The EOMIP-CCSD method is equivalent to the Fock-space multireference coupled cluster method based on single and double excitations (FSMRCCSD) when the latter is applied to singly ionized states.
- <sup>43</sup>J. F. Stanton, *Chem. Phys. Lett.* **237**, 20 (1995).
- <sup>44</sup>J. F. Stanton and N. S. Kadagathur, *J. Mol. Struct.* **376**, 469 (1996).
- <sup>45</sup>J. C. Saeh and J. F. Stanton, *J. Chem. Phys.* **111**, 8275 (1999).
- <sup>46</sup>R. Kobayashi *et al.*, *J. Chem. Phys.* **95**, 6723 (1991).
- <sup>47</sup>R. Kobayashi, R. D. Amos, and N. C. Handy, *Chem. Phys. Lett.* **184**, 195 (1991).
- <sup>48</sup>J. Gauss, J. F. Stanton, and R. J. Bartlett, *J. Chem. Phys.* **95**, 2623 (1991).
- <sup>49</sup>J. F. Stanton and J. Gauss, *J. Chem. Phys.* **101**, 8938 (1994).
- <sup>50</sup>J. F. Stanton and J. Gauss, in *Recent Advances in Coupled-Cluster Methods*, edited by R. J. Bartlett (World Scientific, Singapore, 1997), pp. 49–79.
- <sup>51</sup>J. Gauss and J. F. Stanton, *Chem. Phys. Lett.* **276**, 70 (1997).
- <sup>52</sup>P. G. Szalay, J. Gauss, and J. F. Stanton, *Theor. Chim. Acta* **100**, 5 (1998).
- <sup>53</sup>J. F. Stanton, J. Gauss, J. D. Watts, W. J. Lauderdale, and R. J. Bartlett, ACES II, 1993. The package also contains modified versions of the MOLECULE Gaussian integral program of J. Almlöf and P. R. Taylor, the ABACUS integral derivative program written by T. U. Helgaker, H. J. Aa. Jensen, P. Jørgensen, and P. R. Taylor, and the PROPS property evaluation integral code of P. R. Taylor.
- <sup>54</sup>D. Feller, E. S. Huyser, W. T. Borden, and E. R. Davidson, *J. Am. Chem. Soc.* **105**, 1459 (1983).
- <sup>55</sup>P. Ayala and H. B. Schlegel, *J. Chem. Phys.* **108**, 7560 (1998).
- <sup>56</sup>E. H. Kim, S. E. Bradforth, D. W. Arnold, R. B. Metz, and D. M. Neumark, *J. Chem. Phys.* **103**, 7801 (1995).
- <sup>57</sup>P. E. M. Siegbahn, *J. Comput. Chem.* **6**, 182 (1985).
- <sup>58</sup>R. D. Davy and H. F. Schaefer, *J. Chem. Phys.* **91**, 4410 (1989).
- <sup>59</sup>T. Ishiwata, I. Fujiwara, Y. Naruge, K. Obi, and I. Tanaka, *J. Phys. Chem.* **87**, 1349 (1983).
- <sup>60</sup>T. Ishiwata, I. Tanaka, K. Kawaguchi, and E. Hirota, *J. Chem. Phys.* **82**, 2196 (1985).
- <sup>61</sup>R. R. Friedl and S. P. Sander, *J. Phys. Chem.* **91**, 2721 (1987).
- <sup>62</sup>A. Weaver, D. W. Arnold, S. E. Bradforth, and D. M. Neumark, *J. Chem. Phys.* **94**, 1740 (1991).
- <sup>63</sup>The harmonic frequency of ca. 250 cm<sup>-1</sup> cited in the text is inferred from parameters of a linear vibronic coupling method used in Ref. 62 to fit vibrational levels in the e' mode. The parameters recommended in that work ( $\lambda=0.29$  eV,  $\Delta E=1.87$  eV,  $f_0=0.1$  eV) give an adiabatic potential with  $\omega_4=256$  cm<sup>-1</sup>.
- <sup>64</sup>G. Hirsch, R. J. Buenker, and C. Petrongolo, *Mol. Phys.* **73**, 1085 (1991).
- <sup>65</sup>A. Weaver, R. B. Metz, S. E. Bradforth, and D. M. Neumark, *J. Chem. Phys.* **90**, 2070 (1989).
- <sup>66</sup>S. Mahapatra, H. Köppel, and L. S. Cederbaum, *J. Chem. Phys.* **110**, 5691 (1999).
- <sup>67</sup>P. G. Szalay, M. Nooijen, and R. J. Bartlett, *J. Chem. Phys.* **103**, 281 (1995).
- <sup>68</sup>H. Koch and P. Jørgensen, *J. Chem. Phys.* **93**, 3333 (1990).
- <sup>69</sup>H. Koch, H. J. Aa. Jensen, P. Jørgensen, and T. Helgaker, *J. Chem. Phys.* **93**, 3345 (1990).
- <sup>70</sup>There is also a term that is formally quadratic in the derivative  $\hat{T}$  amplitudes which contributes to the second derivative of the CC energy. This term is responsible for the unphysical behavior that is seen beyond the singularity in the plot of force constant vs coordinate in Fig. 1. It should be noted that this term has also been discussed within the context of the so-called quadratic EOM-CC approach to second-order properties [S. A. Perera, M. Nooijen, and R. J. Bartlett, *J. Chem. Phys.* **104**, 3290 (1996)]. When the state of interest lies just above that which interacts with it, negative force constants can be found at the CC level. This is in contrast to the first-order pole structure which must be followed in an exact theory. Analysis of the CC second derivative expression shows that this unphysical term vanishes in the limit that the two states are related by a pure single excitation and is expected to be small when there is not a significant contribution from double excitations (Ref. 75). A very limited set of exploratory calculations suggests that the effects of this term are found only near the singularity in such cases, when the gap between the two states is smaller than the vibronic coupling strength. A more detailed exposition of these effects will be published in the future.
- <sup>71</sup>J. T. Golab, D. L. Yeager, and P. Jørgensen, *Chem. Phys. Lett.* **78**, 175 (1983).
- <sup>72</sup>H. Koch, R. Kobayashi, and P. Jørgensen, *Int. J. Quantum Chem.* **49**, 835 (1994).
- <sup>73</sup>The substantial differences observed here between the UHF-EOM-CCSD and B-CCD-LR excitation energies do not occur for other, more well-behaved cases such as the lowest-excited states of H<sub>2</sub>O and CH<sub>2</sub>O or the CH<sub>3</sub> and NH<sub>2</sub> radicals.
- <sup>74</sup>Of course, this is not the only difference between B-CC and standard CC methods, as the numerators (which represent approximations to vibronic coupling strengths) are also different from those involving coupling of the reference and EOM states in the latter. In addition, there is clearly a second-order contribution between force constants and B-CC ER matrix eigenvalues that can be seen in Fig. 1. Although the mathematical structure of the B-CC second derivative equations is extremely complicated and has not been analyzed in detail, limited empirical evidence suggests that the second-order contribution to B-CC force constants is somewhat larger than that for standard CC methods.
- <sup>75</sup>J. F. Stanton (unpublished).